A critical GxxxA motif in the γ_6 calcium channel subunit mediates its inhibitory effect on Cav3.1 calcium current

Zuojun Lin[1], Katja Witschas[2], Thomas Garcia[1], Ren-Shiang Chen[1], Jared P. Hansen[1], Zachary M. Sellers[1,3], Elza Kuzmenkina[2], Stefan Herzig[2] and Philip M. Best[1,3]

[1]*Department of Molecular and Integrative Physiology, University of Illinois at Urbana-Champaign, Urbana, IL 61801, USA*
[2]*Department of Pharmacology and Center for Molecular Medicine, University of Cologne, 50931 Cologne, Germany*
[3]*College of Medicine, University of Illinois at Urbana-Champaign, Urbana, IL 61801, USA*

The eight members of the calcium channel γ subunit family are integral membrane proteins that regulate the expression and behaviour of voltage and ligand gated ion channels. While a subgroup consisting of γ_2, γ_3, γ_4 and γ_8 (the TARPs) modulate AMPA receptor localization and function, the γ_1 and γ_6 subunits conform to the original description of these proteins as regulators of voltage gated calcium channels. We have previously shown that the γ_6 subunit is highly expressed in atrial myocytes and that it is capable of acting as a negative modulator of low voltage activated calcium current. In this study we extend our understanding of γ_6 subunit modulation of low voltage activated calcium current. Using engineered chimeric constructs, we demonstrate that the first transmembrane domain (TM1) of γ_6 is necessary for its inhibitory effect on Cav3.1 current. Mutational analysis is then used to identify a unique GxxxA motif within TM1 that is required for the function of the subunit strongly suggesting the involvement of helix–helix interactions in its effects. Results from co-immunoprecipitation experiments confirm a physical association of γ_6 with the Cav3.1 channel in both HEK cells and atrial myocytes. Single channel analysis reveals that binding of γ_6 reduces channel availability for activation. Taken together, the results of this study provide both a molecular and a mechanistic framework for understanding the unique ability of the γ_6 calcium channel subunit to modulate low voltage activated (Cav3.1) calcium current density.

(Received 3 July 2008; accepted after revision 18 September 2008; first published online 25 September 2008)
Corresponding author P. M. Best: 524 Burrill Hall, MC-114, 407 South Goodwin Avenue, Urbana, IL 61801, USA. Email: pbest@illinois.edu

Calcium channel γ subunits comprise a family of eight proteins that share a common topology consisting of four transmembrane domains with intracellular N- and C-terminal ends. The first member of this protein family to be described, γ_1, was isolated as a subunit of the high-voltage activated (HVA), Cav1.1 calcium channel found in skeletal muscle (Jay *et al.* 1990). Unlike other calcium channel accessory subunits (β, $\alpha_2\delta$) which enhance calcium current, γ_1 was shown to accelerate L-type calcium current activation and inactivation in heterologous systems when coexpressed with the Cav1.2 (also an HVA) α_1 subunit (Singer *et al.* 1991; Eberst *et al.* 1997). Skeletal muscle isolated from knockout mice lacking the γ_1 gene have increased HVA calcium current density confirming a physiological role of γ_1 as a negative regulator of HVA, L-type calcium current density in developing skeletal myocytes (Freise *et al.* 2000; Held *et al.* 2002).

Phylogenetic and sequence homology analysis indicates that the recently described γ_6 protein is the closest homologue of γ_1 within the γ subunit family (Burgess *et al.* 2001; Chu *et al.* 2001). Both γ_1 and γ_6 have short C-terminal regions that lack the consensus PDZ1-binding motif that is a notable characteristic of the four γ subunits (γ_2, γ_3, γ_4 and γ_8) known collectively as the TARP proteins that regulate AMPA receptor trafficking and function (Tomita *et al.* 2003; Osten & Stern-Bach, 2006). The γ_1 and γ_6 subunits also share similarities in their tissue distribution since both are expressed primarily or exclusively in striated muscle. As mentioned, the γ_1 subunit was originally isolated from skeletal muscle and its expression seems largely limited to that tissue. mRNA encoding the γ_6 subunit is robustly expressed in cardiac myocytes as two distinct isoforms of varying length and mRNA encoding the full length isoform of γ_6 is also expressed in skeletal muscle (Chu *et al.* 2001). Given the similarities in sequence and tissue distribution between γ_1 and γ_6, it seemed likely that the γ_6 subunit might share with γ_1 an ability to modulate myocyte calcium current. This prediction was recently confirmed. Co-expression of

DOI: 10.1113/jphysiol.2008.159111

the γ_6 subunit cloned from cardiac muscle with α3.1, the pore forming subunit of an low-voltage-activated (LVA) calcium channel expressed in the heart, dramatically decreases calcium current (Hansen *et al.* 2004). The other γ subunits found in cardiac myocytes (γ_4, γ_7) do not cause an inhibition of Cav3-dependent calcium current, a finding that is consistent with the prediction that the γ_6 subunit shares with γ_1 unique functional effects on myocyte calcium channels.

In this study, we extend the electrophysiological analysis of γ_6 to demonstrate that the protein regulates LVA calcium current in native cardiac myocytes as well as in cell lines and to identify critical sequences and structural features within the γ_6 subunit that are involved in its modulation of LVA calcium current. The results reveal that a critical GxxxA motif within TM1 is required for its inhibitory effect on calcium current. To further define the nature of the interaction between γ_6 and α3.1 we performed co-immunoprecipitation experiments that confirm their physical association in both HEK 293 cells and cultured atrial myocytes. Our results indicate that while γ_6 is capable of binding to α3.1, this interaction is not dependent on the GxxxA motif in TM1 that is required for current inhibition. At the level of single channels, we found that interaction with γ_6 causes reduction of the channel availability for activation, which accounts for the decrease of the current density observed in whole-cell experiments. The gating parameters of activation and inactivation, as well as the unitary current through Cav3.1 channels, were not affected by γ_6. Mechanistically, the effect of γ_6 can be explained either by stabilization of the existing non-available state of Cav3.1 or by introduction of a new protein conformation, which is blocked from activation by γ_6.

Methods

Ethical approval

All experimental protocols and animal husbandry were approved and monitored by the Institutional Animal Care and Use Committee and the Division of Animal Resources at the University of Illinois, Urbana-Champaign.

Cell culture

Stably transfected HEK 293 cells expressing the Cav3.1 current were grown at 37°C in Dulbecco's modified Eagle's medium (DMEM; Invitrogen, Carlsbad, CA, USA) with 10% fetal bovine serum (Invitrogen), 1% penicillin/streptomycin in 5% CO_2. Geneticin (G418) was added at a concentration of 200 μg ml^{-1} for selection of transfected cells. Cells having a low passage number (< 20) were used and were maintained in 25 cm^2 culture flasks. Medium was renewed every 24–48 h. The cells were dissociated from the flasks with a 0.05% room temperature trypsin–EDTA solution for 3 min and suspended with medium for low density re-plating every 4–6 days. During re-plating, a fraction of the cells were plated on 35 mm culture dishes, which were then used for transfection and electrophysiology. Cells were again trypsinized and re-suspended in bath solution prior to electrophysiological recording. For single channel analysis, native HEK 293 cells were cultured similarly except that the growth medium was not complemented with G418.

Adult rat atrial myocytes were isolated from 21- or 22-day-old Sprague–Dawley rats anaesthesized using 4% isoflurane (Baxter, Deerfield, IL, USA) and a protocol modified from our previous procedure (Piedras-Renteria *et al.* 1997). Following anaesthesia, cardiac contraction was stopped by injecting a cardioplegic solution. The heart was removed and the atria isolated and digested using a solution containing 0.3–0.4 mg ml^{-1} collagenase B (Roche, Indianapolis, IN, USA) inside a stirred vial for 30–35 min at 37°C. The tissues were then transferred to a recovery solution and cut into small pieces. Single cells were released by pipetting/trituration using a fire-polished glass pipette. After sitting at room temperature for 1 h, the cells were then plated in the culture medium (1 : 1 with DMEM containing Ham's F-12, 4 nM insulin, 2% penicillin/streptomycin, 2.5 mg ml^{-1} bovine serum albumin, 1 nM selenium, 1 nM thyroxine, 5 μg ml^{-1} transferrin, 10 nM testosterone) supplemented with 10% fetal bovine serum (Invitrogen) and 10 μM cytosine arabinoside (Sigma-Aldrich, St Louis, MO, USA). Culture vessels were precoated with 10 μg ml^{-1} collagen I (Roche) and 5 μg ml^{-1} fibronectin (Sigma-Aldrich). For electrophysiology experiments the cells were plated on coverslips. Cells were kept in a humidified incubator with 5% CO_2 at 37°C until use.

Molecular cloning and γ constructs

The coding regions of rat γ_1, γ_4, γ_6, γ_{6S} and γ_7 (Chu, Robertson *et al.* 2001) as well as those of all chimeric cDNAs were subcloned into pCR II vectors (Invitrogen) by TA cloning. The accession numbers of these previously described genes are as follows: rat γ_1 (NM_019255), rat γ_4 (AF361341), rat γ_6 (AF361343), rat γ_{6S} (AF361344), and rat γ_7 (AF361345). The chimeras created are shown schematically in Fig. 1 and in translated amino acid sequence as follows: γ6444 (γ_6 1–98/γ_4 74–327); γ4446 (γ_4 1–159/γ_6 193–260); γ6446 (γ_6 1–99/γ_4 75–159/γ_6 193–260); γ6664 (γ_6 1–201/γ_4 177–327); γ4666 (γ_4 1–105/γ_6 141–260); γ4.6666 (γ_4 1–10/γ_6 1–260); γ_6 N-trunc (γ_6 32–260); γ_6 N-del (γ_6 41–260); γ_4 C-trunc (γ_4 1–239). From pCR II vectors, rat γ_1, γ_4, γ_6, γ_{6S}, γ_7, and chimeric subunit cDNAs were then transferred to the

expression vector AdCGI, as previously described (Hansen *et al.* 2004). From the AdCGI γ_1 and AdCGI γ_6 constructs, mutants of γ_1 and γ_6 were created with the Stratagene QuikChange II Site-Directed Mutagenesis Kit (Stratagene, La Jolla, CA, USA), as per the manufacturer's instructions and primer design programme. For immunoprecipitation studies involving amino-terminal FLAG-tagged γ subunits, cDNAs were transferred from the AdCGI constructs to the pFLAG-CMV-2 vector (Sigma-Aldrich).

Transfection

HEK 293 cells stably transfected with the Cav3.1 subunit were transiently transfected, at 50–70% confluency, with a bicistronic vector encoding both GFP and γ subunit cDNAs using Lipofectamine 2000 reagent (Invitrogen) as per the manufacturer's recommendations. Cells were visualized using a Nikon inverted microscope with a FITC filter. Cells for immunoprecipitation were transfected with a vector encoding amino-terminal FLAG-tagged fusion proteins.

For single-channel analysis, native HEK 293 cells were transiently transfected with a mixture of vectors using Effectene Reagent (Qiagen, Hilden, Germany) according to the manufacturer's protocol. Mixtures contained pcDNA3.1 plasmid with a Cav3.1 gene (generously provided by Professor Edward Perez-Reyes, Charlottesville, VA, USA) and pGFP, AdCGI, AdCGI γ_6 or AdCGI γ_7 vector in mass ratios of 1 : 1 or 1 : 3. The total DNA amount was 1 μg. Reporter pGFP vector was from Clontech (Palo Alto, CA, USA); the GeneBank accession number is U19280.

As an exception, for single-channel conductance measurements, we used HEK 293 cells stably expressing Cav3.1 channels. If needed, the cells were transiently transfected with AdCGI γ_6 vector using Effectene Reagent.

Adenovirus infection

Recombinant adenovirus expressing amino-terminal FLAG-tagged γ_6 (AdFLAGγ_6) was generated through the pAdEasy system (Q.biogen, Carlsbad, CA, USA). Empty recombinant adenovirus (Empty Ad) was obtained as a gift from Dr Yang Xiang, University of Illinois at Urbana-Champaign. Viral titre for each virus was obtained through optical density as recommended by the manufacturer (Q.biogen). Following atrial myocyte isolation, primary cultures were cultured for 48 h before medium replacement and addition of viruses at varying multiplicities of infection (m.o.i.). We adjusted the m.o.i. for the viruses so that, after 48 h of infection, there was no change in total Cav3.1 protein (Fig. 5*C*) due to non-specific effects, as compared to no virus treatment (data not shown). The myocytes were incubated with virus-containing medium for an additional 48 h before being used for subsequent experiments.

Immunoprecipitation and immunodetection

HEK 293 cells and cultured atrial myocytes were processed for immunoprecipitation assay and immunoblot analysis 24–48 h post-transfection/infection. Cells were washed and scraped from flasks with ice cold PBS (without Ca^{2+} or Mg^{2+}) and centrifuged for 5 min at 500 *g* at 4°C. Cell pellets were resuspended in 1.0 ml lysis buffer (50 mM Tris HCl, 150 mM NaCl, 1 mM EDTA, 2% Triton X-100, and 1 : 100 Protease Inhibitor Cocktail Set III (EMD Biosciences, San Diego, CA, USA) and incubated with

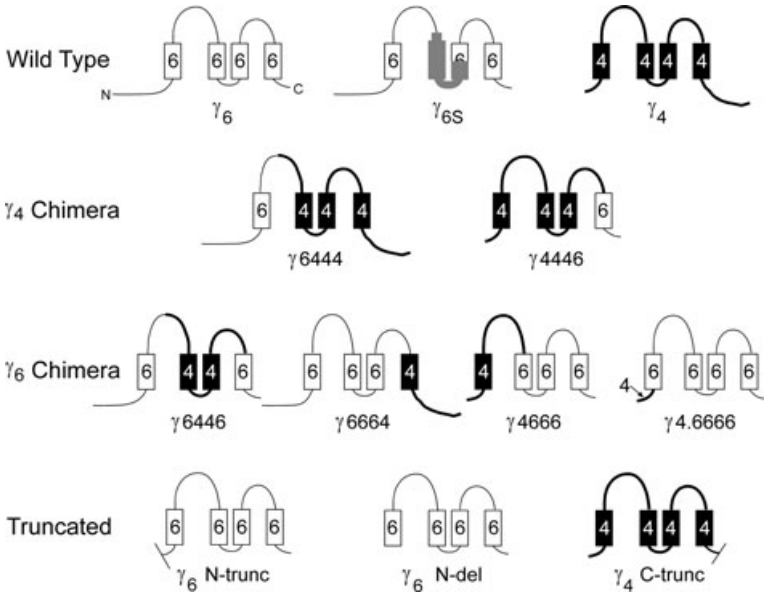

Figure 1. Schematic representations of chimeric and truncated γ subunits used in this study
Chimeric γ subunits were engineered to identify specific regions within the γ_6 subunit that are required for its ability to reduce Cav3.1 calcium current density. Numbers in the diagrams indicate the γ isoform from which each fragment was derived. γ_6 fragments are in white boxes and thin lines, while γ_4 fragments are in black boxes and thick lines. Grey colour indicates the naturally deleted sequence in γ_{6S}. Note that the γ_4 subunit has no functional effect on Cav3.1 current density. Truncated subunits were used to probe the importance of C- and N-terminal cytoplasmic regions.

constant mixing for 1 h at 4°C. Samples were cleared by centrifugation at 10 000 *g* for 2 min at 4°C and protein concentrations determined through the Bradford assay. Equal protein amounts of cell lysate were added to a 75 μl bed volume of anti-FLAG M2 affinity gel (Sigma-Aldrich) that was washed three times with lysis buffer. Samples were immunoprecipitated with constant mixing overnight at 4°C. Beads were washed three times with lysis buffer and incubated in sample buffer containing 1% SDS, 50 mM DTT, and 10% glycerol for 30 min at 25°C. Protein samples were separated from the beads and transferred to new tubes with polyethylene spin columns (Pierce, Rockford, IL, USA). Equal amounts of cell lysate and immunoprecipitate were separated by SDS-PAGE on 6% or 12% polyacrylamide gels containing 0.4% SDS. Samples were transferred to PVDF membrane and immunoblotted. For detection of Cav3.1 and the FLAG epitope, polyclonal anti-Cav3.1 antibody (Alomone Laboratories, Jerusalem, Israel) and polyclonal anti-FLAG antibody (Sigma-Aldrich) were used, respectively, both at 1 : 1000 dilution. Horseradish peroxidase (HRP)-conjugated goat anti-rabbit IgG secondary antibody (Zymed, South San Francisco, CA, USA) was used at 1 : 20 000 dilution. Chemiluminescent detection was performed using ECL reagent (Amersham Biosciences, Piscataway, NJ, USA). Pixel densitometry was performed through ImageQuant 5.2 (GE Healthcare, Piscataway, NJ, USA). Integrated intensity values of all the pixels in a box drawn around a band, minus the background were obtained. 'Total' is defined as the sum of all band values in a gel from a given trial and 'percentage of total' values were calculated for each band per trial allowing comparison across different gels from multiple trials. The same size box was used for each band in a given gel from a given trial. The ratio of percentage of total Cav3.1 in the immunoprecipitate (IP) to percentage of total FLAG γ protein in the IP was calculated for each sample in a trial. Ratios were then averaged and scaled such that the FLAGγ6 group would represent 100%.

Electrophysiology

Whole cell Ca^{2+} currents were recorded using an Axopatch-1D amplifier and Clampex 8.0 software (Molecular Devices/Axon Instruments, Union City, CA, USA). Pipettes were made from boroscillicate glass and had typical resistances of 2–4 MΩ. For HEK 293 cell recordings, the pipette solution contained (in mM): 130 NaCl, 10 EGTA, 2 or 5 $MgCl_2$, 1 $CaCl_2$, 10 Hepes, 3 Tris-ATP, and 0.3 Li_2GTP. Two different bath solutions were used. The first, used for experiments with γ subunit chimeras, contained (in mM): 130 NaCl, 1 $MgCl_2$, 2 $CaCl_2$, 10 glucose, 10 Hepes and 0.03 TTX. The second, used for experiments with γ subunit containing point mutations, contained (in mM): 137 NaCl, 1 KCl, 1 $MgCl_2$, 0.33 NaH_2PO_4, 2 $CaCl_2$, 10 Hepes. All solutions were adjusted to pH 7.4 with NaOH and 280 mosmol l^{-1} with sucrose. No Cl^- currents were evident in any HEK 293 cells line, stably transfected or not, and no attempt was made to eliminate Cl^- currents from data records.

Several different protocols were used to determine the biophysical characteristics of currents in HEK 293 cells. The voltage dependence of activation was determined using tail currents at −60 mV upon stepping back from test potentials ranging from −90 mV to +60 mV with various pulse durations that corresponded to the time to peak current measured at the corresponding test potentials. The voltage dependence of inactivation was measured by stepping the cells to voltages ranging from −120 mV to 50 mV for 500 ms to inactivate the Ca^{2+} channels. After this conditioning step the membrane was returned to the holding potential briefly (3 ms) before being depolarized a second time to +20 mV for 150 ms during which time the peak current was measured. Time constants for inactivation were measured by fitting a single exponential equation to the decay phase of currents elicited by voltage steps from −50 to +30 mV from a holding potential of −100 mV. Time constants for deactivation were measured by fitting either a single or a double exponential to the decay phase of tail currents.

To account for the inherent variation in calcium current density in the HEK-Cav3.1 stable cell line, the averaged current density of each test group of cells was normalized to the mean current density of a control group of cells. A minimum of five cells (typically 7–10) from each group was used to calculate the mean current densities of test and control cells. At least two independent transfections were performed for each test condition.

For recordings in atrial myocytes, the pipette solution contained (in mM): 120 CsCl, 10 Cs-EGTA, 5 $MgCl_2$, 1 $CaCl_2$, 10 Hepes, 3 Tris-ATP and 0.3 Tris-GTP, pH 7.4 with CsOH. The bath solution contained (in mM) 135 CsCl, 5 $CaCl_2$, 1 $MgCl_2$ and 10 Hepes, pH 7.4 with CsOH. All solutions were adjusted with sucrose to 280–290 mosmol l^{-1} as needed.

Total calcium currents in myocytes were elicited by stepping the membrane voltage to test pulses between −70 and +70 mV for 50 ms from a holding potential of −100 mV every 3 s. For high-voltage-activated (HVA) currents, the holding potential was set at −50 mV to inactivate LVA currents. The LVA currents were obtained by subtracting the HVA traces from the total calcium traces at corresponding test potentials. To minimize the influence of current rundown on the results, initial measures of HVA and LVA currents were performed at test potentials of 0 and −40 mV, respectively, before an entire current–voltage relationship was obtained.

All current records were adjusted for junctional potential and pipette capacitance. Series resistance was

compensated to $>80\%$. Currents were digitized at 10–40 kHz and filtered at 2–10 kHz. In some cases, current–voltage relationships were recorded using an on-line P/−4 subtraction procedure to eliminate linear capacitative and leakage currents.

All data are reported as means ± standard error of the mean (S.E.M.). Mean values were tested for statistical significance using single factor ANOVA when appropriate with a P value of 0.05.

Single channel analysis

Single Cav3.1 channels were measured in the cell-attached configuration using an Axopatch-1D amplifier and pCLAMP 5 software (Molecular Devices/Axon Instruments). The bath solution contained (in mM): 120 potassium L-glutamate, 25 KCl, 10 glucose, 2 EGTA, 2 $MgCl_2$, 1 $CaCl_2$, 10 Hepes, 1 Na_2ATP, pH 7.2 with KOH. High potassium concentration in the bath solution served to nullify the resting potential of HEK 293 cells. Pipettes had typical resistance of 5–7 MΩ and were coated with Sylgard (Dow Corning, Midland, MI, USA). The pipette solution contained (in mM): 110 $BaCl_2$ and 10 Hepes, pH 7.3 with TEA-OH. Unless otherwise stated, Ba^{2+} currents were elicited by depolarizing voltage steps to −20 mV from a holding potential of −90 mV (test pulse duration 147.9 ms, repetition rate 0.5 Hz), filtered at 2 kHz with a 4-pole Bessel filter, and sampled at 10 kHz. Measurements which lasted less than 180 sweeps were discarded.

Single-channel data were analysed using Fetchan and pStat programs (pCLAMP 6, Molecular Devices/Axon Instruments). Linear leak and capacity transients were digitally subtracted from recordings.

Channel opening and closures were determined by the half-height criterion. The maximal number of simultaneous openings was used as an estimate of the number of channels in the patch, n_{ch}. Only patches with $n_{ch} \leq 3$ were analysed.

Sweeps that contained no openings were termed blank sweeps, as opposed to the so-called active sweeps in which at least one channel opening was detected. Channel availability (f) was defined as the ratio of the number of active sweeps (M_a) to the number of all sweeps (M). For several channels in the patch, channel availability was calculated as (Michels *et al.* 2002):

$$f = 1 - \sqrt[[n_{ch}]]{1 - M_a/M}$$

Mean observed open time (t_O) was determined as the sum of the times spent by channels in the open state divided by the number of openings. Open probability within active sweeps ($P_{O,active}$) was calculated as the full open probability divided by the channel availability, where the full open probability was the sum of the times spent by channels in the open state divided by the number of channels and the total length of the test pulses.

Unitary current amplitude (i_O) was calculated as the time-average of the current in the open state. Average current traces were constructed by summing currents through open states at a given time point after a depolarization, and dividing them by the number of sweeps and the number of channels. The peak of the average current (I_{peak}) and the average current at the end of the pulse (I_{end}) were used to calculate the extent of the inactivation as $1 - I_{end}/I_{peak}$.

To address dynamics of the transitions between available and non-available states, we performed 'runs analysis' (Horn *et al.* 1984; Nilius, 1988). First, we tested whether blank and active sweeps occurred randomly (Bernoulli trials) or were clustered together. The latter case implies existence of separate non-available and available states with slow transitions between them. The sequences of consecutive blank and active sweeps were termed blank and active runs, respectively. For a Bernoulli process, when the number of sweeps $M > 40$, the exact distribution of the observed number of runs (R) approaches an asymptotic distribution, and a standardized random variable Z_R with a mean of 0 and a variance of 1 can be used for statistical tests (Horn *et al.* 1984):

$$Z_R = -\frac{R - 2Mp(1-p)}{2\sqrt{M}p(1-p)},$$

where $p = M_a/M$ is the portion of the active sweeps (the channel availability should be additionally corrected for the number of channels). In the case of clustering, R will be less than the expected number of sweeps, $2Mp(1-p)$, forming a positive Z_R. Z_R values > 1.64 are considered to be statistically significant ($P < 0.05$, one-tailed test) (Horn *et al.* 1984; Nilius, 1988), and indicate a serial dependence for a given measurement. For a sample of measurements, Z_R values were compared with 0 using Student's t test (one-tailed).

After the serial dependence of the channel availability had been proved, the lifetimes of the available and non-available states were estimated as follows. For simplicity, we assumed a kinetic scheme with a single available (A) and a single non-available (N) state, which manifest themselves in active and blank sweeps, respectively. The transition rates from A to N and from N to A are, correspondingly, $k_{A\to N}$ and $k_{N\to A}$. The distribution of the lengths of the blank runs forms a geometrical distribution, such that the probability to observe a run of $r+1$ sweeps equals the probability to observe a run of r sweeps times $p_{N\to N}$, where $p_{N\to N}$ is the probability to observe a blank sweep given the previous sweep was blank. The average length of the blank runs, l_B, is then $1/(1 - p_{N\to N})$. For our kinetic scheme, $p_{N\to N} = \{f e^{-(k_{N\to A}+k_{A\to N1})t} + (1-f)\}^{n_{ch}}$, where t is the

time between sweeps, i.e. 2 s. The terms in braces are the solution of the differential equations for one channel; the power of n_{ch} arises because the probability to be in the blank state is the product of the probabilities to be in the blank state for every channel. Using the ratio $k_{N\to A}/k_{A\to N} = f/(1-f)$, one obtains for the life times of the non-available and available states, $\tau_N = 1/k_{N\to A} = \frac{f}{\ln \frac{f}{\sqrt[n_{ch}]{1-1/I_B}-(1-f)}}$ and $\tau_A = 1/k_{A\to N} = \tau_N f/(1-f)$, respectively.

Finally, we compared single-channel slope conductance of Cav3.1 channels without and with γ_6 subunit. In these measurements, patches were held at −90 mV and Ba^{2+} currents were evoked by voltage steps to −30, −20, −10, 0 and 10 mV. Only patches where the measurements were successful at two or more membrane voltages separated by 30 mV, were analysed. Slope conductance values were estimated by linear regression of unitary current amplitudes at different potentials.

All single channel data are reported as means ± S.E.M. Statistical significance between groups was assessed by single factor ANOVA. Linear regression analysis was performed using a γ_6 to Cav3.1 DNA mass ratio as an independent variable. For Cav3.1 + AdCGI, Cav3.1 + pGFP, and Cav3.1 + γ_7, the value of the independent variable was zero. In the runs analysis, Z_R values were tested as described above.

Results

Effects of γ subunit chimeras on Cav3.1 current density

We have previously shown that coexpression of the γ_6 subunit in HEK cells stably transfected with the α3.1 subunit causes a significant decrease in Cav3.1 calcium current density when compared to the expression of α3.1 alone (Hansen *et al.* 2004; also see Fig. 4 this paper). This inhibitory effect is unique to the γ_6 isoform as no inhibition is seen with γ_4 or γ_7. We have also shown that γ_{6S}, the short isoform of γ_6, has the same effect on Cav3.1 calcium current as the full-length γ_6. The γ_{6S} isoform is missing all of the second transmembrane domain and much of the third transmembrane domain of the full-length protein (Fig. 1). Therefore sequence motifs that are required for the unique ability of γ_6 to decrease Cav3.1 current density must be found outside of the central core of the protein.

To confirm this prediction, a chimeric subunit was engineered that combined the N- and C-terminal regions of γ_6 (including TM1 and TM4 and the associated cytoplasmic tails) with TM2 and TM3 from γ_4. This construct, γ6446, was then transfected into HEK-Cav3.1 cells and the calcium current density compared to that of positive controls transfected with wild-type γ_6 (which show decreased current) and negative controls transfected with γ_4 (in which current is unaffected). Current density in the cells transfected with γ6446 was reduced significantly ($19 \pm 4\%$; $n = 10$; $P < 0.01$) compared to control values (Fig. 2). This result confirms the prediction that replacement of TM2 and TM3 of γ_6 with the homologous regions from γ_4 does not alter its ability to inhibit calcium current. It also indicates that the critical portion(s) of γ_6 must be contained in the N- or C-terminal regions.

To probe the importance of the terminal regions of γ_6, a series of chimeric γ proteins was designed in which the N- and C-terminal regions were targeted for substitution or truncation (Fig. 1). The first set of chimeras was designed to determine whether either the N-terminal or the C-terminal region of γ_6 was sufficient for current inhibition or whether both regions were required simultaneously. The chimera γ6444 was engineered using wild-type γ_4 but with the N-terminal region replaced by the homologous region of γ_6. The substituted region contained the N-terminal cytoplasmic domain, TM1 and a portion of the extracellular region linking TM1 to TM2. The second chimera in this series, γ4446, was also based on wild-type γ_4 but in this case TM4 and the C-terminal cytoplasmic domain from γ_6 were substituted into the protein. When expressed in the HEK-Cav3.1 cells, γ6444 decreased normalized current density to $46 \pm 7.6\%$ ($n = 12$, $P < 0.05$) of control values (Fig. 2). The magnitude of this effect is similar to that seen for wild-type γ_6. In contrast, cells transfected with γ4446 expressed calcium currents with densities similar to those obtained in controls ($100\% \pm 15\%$, $n = 7$, $P > 0.05$) as was the case with wild-type γ_4 (Fig. 2). These results indicate that the N-terminal region of γ_6, including the cytoplasmic region and TM1, is necessary for the inhibition of LVA calcium current.

To confirm this result and to rule out any effects of using the wild-type γ_4 as the backbone for construction of the chimeras, we engineered proteins using wild-type γ_6 into which TM1 and TM4 of γ_4 were substituted for the homologous regions of γ_6 (γ6664, γ4666). In the case of the γ6664 chimera, the construct contained the cytoplasmic C-terminal region as well as TM4 of γ_4. The γ4666 construct contained the N-terminal cytoplasmic region, TM1 and part of the extracellular region linking TM1 and TM2 from γ_4. Calcium current density in cells transfected with γ4666 was not statistically different from controls ($82 \pm 6\%$, $n = 9$, $P > 0.05$) (Fig. 2). In contrast, the calcium current density in cells transfected with γ6664 was significantly reduced ($37 \pm 5\%$, $n = 9$, $P < 0.01$) (Fig. 2). These results are consistent with the previous finding that the N-terminal region of γ_6 is critical for the inhibitory effect of this isoform on calcium current density.

To define more precisely what portion of the N-terminal region is responsible for this effect, we engineered additional γ_6 subunits that had portions of the N-terminal cytoplasmic domains removed (Fig. 1). The construct γ_6 N-trunc had the first 30 amino acids deleted leaving a short (9 amino acid) cytoplasmic sequence before TM1. A similar construct, γ_6 N-del, had the entire N-terminal cytoplasmic region up to TM1 deleted from the protein. Finally, γ4.6666 had the N-terminal cytoplasmic domain of γ_6 replaced by the homologous region of γ_4. Expression of all of these constructs significantly decreased calcium current densities (Fig. 2). The magnitude of the effect was $52 \pm 5\%$ for γ_6 N-trunc ($n = 8$, $P < 0.05$), $22 \pm 3\%$ for γ_6 N-del ($n = 10$, $P < 0.01$) and $29 \pm 5\%$ for γ4.6666 ($n = 10$, $P < 0.01$). These results show that the N-terminal cytoplasmic region of γ_6 is not necessary for the inhibitory effect of this isoform, since it can be removed or replaced with the homologous region of γ_4 without diminishing the effect compared to that of the wild-type.

One major difference between γ_6 and γ_4 is the presence of a C-terminal PDZ-binding domain in γ_4. To determine whether the PDZ-binding domain in γ_4 somehow prevented it from altering calcium current, we constructed a truncated form of γ_4 in which the C-terminal region was deleted (γ_4 C-trunc, Fig. 1). This change had no significant effect on calcium current indicating that differences in the

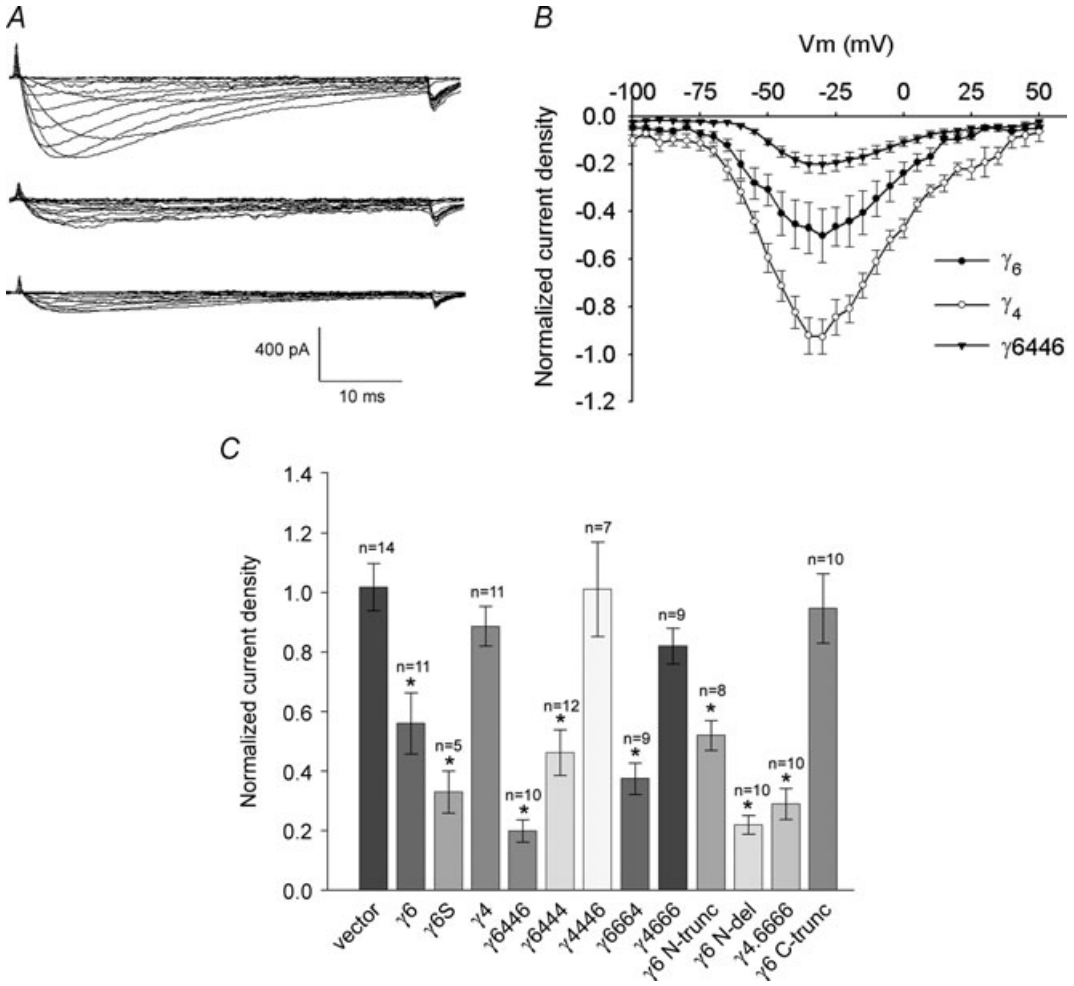

Figure 2. The N-terminal region of γ_6 is required for its inhibitory effect on Cav3.1 calcium current density

A, representational Cav3.1 current traces and *I–V* curves demonstrating the effects of transiently transfecting Cav3.1/HEK cells with plasmids expressing: γ_4 (top), γ_6 (middle) and γ_{6446} (bottom). Calcium currents were elicited by a 50 ms voltage step to between −100 and 50 mV from a holding potential of −100 mV. *B*, typical normalized current voltage curves. The γ_4 subunit does not affect Cav3.1 calcium current and these traces represent negative controls. They are equivalent to currents recorded from untransfected Cav3.1/HEK cells. The chimeric protein γ_{6446} decreases calcium current to an extent similar to that seen with the wild-type γ_{6S}. *C*, a comparison of the effects of the engineered peptides with those of the wild-type indicates that any peptide containing TM1 of γ_6 decreases Cav3.1 current density. Normalized current densities were calculated at −30 mV.

Table 1. Wild-type and chimeric γ subunits do not affect the voltage dependency and kinetics of Cav3.1 current

	I–V curve	Activation		
	V_{peak} (mV)	$V_{0.5}$ (mV)	k	Time to peak at −20 mV (ms)
Vector	−29.5 ± 0.9 ($n = 10$)	−32.3 ± 1.5 ($n = 9$)	13.3 ± 0.3	5.7 ± 0.4
γ_6	−31.1 ± 3.1 ($n = 9$)	−36.6 ± 6.2 ($n = 4$)	12.7 ± 1.5	6.0 ± 0.8
γ_{6S}	−27.0 ± 2.5 ($n = 5$)	−36.6 ± 6.2 ($n = 4$)	12.7 ± 1.5	6.4 ± 0.5
γ_4	−30.6 ± 1.5 ($n = 9$)	−37.3 ± 0.9 ($n = 8$)	11.8 ± 0.5	5.2 ± 0.5
γ6446	−31.3 ± 1.3 ($n = 8$)	−36.0 ± 1.1 ($n = 8$)	10.8 ± 0.6	7.6 ± 2.0
γ6444	−29.5 ± 0.8 ($n = 11$)	−33.2 ± 0.8 ($n = 11$)	12.4 ± 0.4	4.9 ± 0.3
γ4446	−30.0 ± 1.6 ($n = 8$)	−30.8 ± 3.3 ($n = 9$)	11.2 ± 0.7	8.0 ± 1.1
γ6664	−31.9 ± 2.3 ($n = 8$)	−32.9 ± 1.4 ($n = 6$)	12.4 ± 0.7	14.4 ± 4.7
γ4666	−26.6 ± 3.1 ($n = 6$)	−38.0 ± 3.3 ($n = 3$)	12.0 ± 0.8	17.0 ± 5.9
γ_6 N-trunc	−31.6 ± 1.9 ($n = 10$)	−28.3 ± 5.0 ($n = 8$)	13.1 ± 0.8	6.3 ± 0.5
γ_6 N-del	−31.1 ± 2.7 ($n = 9$)	−26.2 ± 2.5 ($n = 9$)	15.0 ± 1.7*	12.1 ± 2.4
γ4.6666	−31.4 ± 1.8 ($n = 7$)	−33.2 ± 2.0 ($n = 6$)	14.9 ± 1.6	6.7 ± 0.9
	Deactivation	Inactivation		
	τ at −100 mV (ms)	$V_{0.5}$ (mV)	k	τ at −20 mV (ms)
Vector	1.19 ± 0.19 ($n = 9$)	−71.9 ± 1.4 ($n = 8$)	5.4 ± 0.1	19.8 ± 1.3
γ_6	1.54 ± 0.48 ($n = 4$)	−78.5 ± 2.6 ($n = 6$)	5.4 ± 0.3	18.6 ± 1.1
γ_{6S}	1.20 ± 0.06 ($n = 3$)	−72.0 ± 5.9 ($n = 3$)	5.9 ± 0.7	22.9 ± 0.7
γ_4	1.84 ± 0.28 ($n = 8$)	−79.2 ± 1.5 ($n = 7$)	6.1 ± 0.2	15.8 ± 0.7
γ6446	1.20 ± 0.15 ($n = 8$)	−75.3 ± 1.2 ($n = 8$)	4.4 ± 0.3	16.4 ± 0.9
γ6444	1.18 ± 0.10 ($n = 9$)	−74.1 ± 0.5 ($n = 11$)	5.2 ± 0.1	16.5 ± 1.1
γ4446	1.69 ± 0.32 ($n = 7$)	−67.0 ± 2.3 ($n = 8$)	5.9 ± 0.5	22.8 ± 3.0
γ6664	1.38 ± 0.26 ($n = 7$)	−73.0 ± 1.7 ($n = 6$)	6.3 ± 0.3	24.9 ± 1.9
γ4666	1.47 ± 0.48 ($n = 4$)	−72.1 ± 1.9 ($n = 3$)	5.8 ± 0.3	23.3 ± 1.1
γ_6 N-trunc	1.41 ± 0.18 ($n = 7$)	−74.0 ± 2.2 ($n = 5$)	5.6 ± 0.1	19.4 ± 1.1
γ_6 N-del	1.24 ± 0.14($n = 9$)	−70.2 ± 0.4 ($n = 9$)	5.0 ± 0.2	25.4 ± 1.0*
γ4.6666	1.39 ± 0.19 ($n = 7$)	−78.1 ± 1.2 ($n = 6$)	5.8 ± 0.2	19.0 ± 1.5

All data were expressed as mean ± S.E.M. The resting and test potentials were −90 mV and −20 mV, respectively. No significant differences in the voltage at peak current, voltage dependency, or kinetic parameters were detected between cells transiently transfected with vector as compared to cells transfected with γ_6, γ_{6S}, γ_4 or any of the chimeras studied except for where noted. *$P < 0.05$

C-terminal region between γ_6 and γ_4 do not explain the difference in their function (Fig. 2).

Taken together, these results demonstrate that TM1 of γ_6 is responsible for the inhibitory effect of this protein on Cav3.1 calcium current.

No effects of γ_6 subunit chimeras on the biophysical properties of macroscopic Cav3.1 calcium current

We have previously shown that the effect of γ_6 on Cav3.1 calcium current is limited to decreasing current density with little change in the voltage dependency and kinetics of the currents (Hansen *et al.* 2004). The results from the present study confirm these previous observations and also indicate that the chimeric γ subunit proteins had little effect on the biophysical properties of the currents (Table 1). For instance, none of the chimeras or truncated forms studied had a significant effect on the voltage at which peak current occurred. In all but one case, no effects were seen on the slope factor (k), nor on the voltage of half-maximal current ($V_{0.5}$) derived from the Boltzmann curve used to fit the voltage dependency of activation. The exception was the γ_6 N-del chimera in which the k of activation was shifted from a control value of 13.3 ± 0.3 to 15.0 ± 1.7 ($P < 0.05$). Similarly, none of the transfected γ subunits or chimeras had a significant effect on $V_{0.5}$ or k of the voltage dependency of inactivation. There were no significant differences in the time to peak current, the time constant of inactivation, or the fast component of the time constant of inactivation for any chimera studied.

A GxxxA motif is required for inhibition of LVA calcium current by γ_6

To identify specific residues or motifs within TM1 of γ_6 that are required for its functional effect, we constructed

γ_6 proteins with targeted amino acid substitutions. The first transmembrane domain of γ_6 is unique in that it contains two GxxxA motifs ($G^{42}xxxA^{46}$ and $G^{49}xxxA^{53}$) (Fig. 3*A* and *B*). (G/A/S)xxx(G/A/S) motifs are known to enable helix–helix interactions between helical domains within proteins. The presence of amino acids with small side chains located one helical turn along the helix axis is thought to provide indentations that promote close association of adjacent helices (Russ & Engelman, 2000). Since we have shown that a helical transmembrane domain is required for the functional effect of γ_6, it is reasonable to hypothesize that helix–helix interactions are a critical aspect of the molecular mechanism underlying its effects. We therefore focused our analysis on the two GxxxA motifs in TM1 of γ_6.

As an initial test to determine whether one or both of the GxxxA motifs within TM1 of γ_6 are, in fact, functionally significant, mutants were created in which the glycine (G) residues at positions 42 and 49 were replaced with either leucine (L, large side-chain) or alanine (A, small side-chain). The goal was to determine whether the presence of small side chains was an obligatory feature of residues at these positions and whether substitution of residues with large side chains would eliminate the subunit's functional effect. When the G42A mutant was expressed, Cav3.1 current density decreased to 73.4% ± 8.9% ($n = 16$) ($P < 0.05$) compared to control, not significantly different from what is seen with coexpression of the wild-type γ_6 (Fig. 3*C*). In contrast, current density in cells expressing the G42L mutant was 107.5% ± 10.9% ($n = 19$) compared with control indicating that the mutant protein had lost its inhibitory function. Thus an amino acid with a small side chain at position 42 appears to be necessary for the inhibitory activity of TM1 of γ_6. To test this idea further we engineered the A46I mutant and found that it lost the inhibitory effect on Cav3.1 current density (Fig. 3*C*). These results demonstrate that a small side chain residue is required at both the Gly42 and Ala46 positions and demonstrates that the complete $G^{42}xxxA^{46}$ motif is necessary for the γ_6 subunit to be effective in altering Cav3.1 calcium current density.

A similar set of substitutions was made in the second GxxxA motif (Fig. 3). Both the G49A and G49L mutants retained the ability to decrease LVA calcium current density (67.6% ± 5.9%, $n = 36$; and 73.1% ± 4.8%, $n = 22$, respectively) indicating that the second GxxxA motif in γ_6 is not functionally significant.

Introduction of a GxxxA motif into γ_1 makes it inhibitory for Cav3.1 current

Wild-type γ_1 does not alter calcium current density when coexpressed with Cav3.1 (Fig. 3*D*) suggesting that the functional effect of γ_1 may be limited to HVA, L-type channels as shown by Campbell and colleagues (Arikkath *et al.* 2003). Unlike TM1 of γ_6, the first TM of γ_1 contains only a single GxxxA motif ($G^{19}xxxA^{23}$) that corresponds with respect to its relative position within the helix to the second motif in γ_6 ($G^{49}xxxA^{53}$). We have demonstrated that the second motif of γ_6 ($G^{49}xxxA^{53}$) is not necessary for the protein to alter LVA calcium current density (Fig. 3*C*). Given the close homology of the γ_1 and γ_6 subunits we hypothesized that introducing a GxxxA motif into TM1 of γ_1 at the same position as the first (functional) motif in γ_6 would make γ_1 inhibitory when coexpressed with α3.1. To test this idea two γ_1 mutants were made. The first (T12G) contained part of the GxxxA motif while the second, double mutant (T12G, I16A) contained the complete motif. When coexpressed with α3.1 the γ_1 double mutant (T12G, I16A) significantly inhibited Cav3.1 current while the single mutant had, like wild-type γ_1, no effect (Fig. 3*D*). Thus introduction of a GxxxA motif at the appropriate position in TM1 of γ_1 imparts a new function to the γ_1 subunit (an ability to modulate Cav3.1 current) that is not seen in the wild-type protein. This result is consistent with our observation that the first GxxxA motif within TM1 of γ_6 is the critical sequence that determines its functional effect on Cav3.1 calcium current.

Interaction of γ_6 and α3.1

We have demonstrated a unique inhibitory effect of γ_6 on Cav3.1 current that is not seen with other γ subunits (Hansen *et al.* 2004). A simple hypothesis to explain this difference is that the γ_6 subunit interacts directly with α3.1 to produce its effect on Cav3.1 calcium current while sequence differences in γ_4 and other γ subunits alter their interactions with α3.1 in some way, making them less effective as regulators of LVA current.

To test this idea we used co-immunoprecipitation as an assay of γ/α3.1 binding. FLAG-tagged γ subunits were transiently expressed in HEK 293 cells that stably expressed α3.1. Cell lysates were immunoprecipitated with FLAG antibody and then probed with anti-Cav3.1 antibody to identify γ/α3.1 complexes. As shown (Fig. 4*A*), there was robust co-immunoprecipitation of γ_6 with α3.1 indicating a strong physical association between these two calcium channel subunits. In contrast, the interaction between α3.1 and γ_4 was significantly reduced, being approximately 10% of γ_6 (Fig. 4*B*). Thus the reduced ability of γ_4 to form a stable complex with α3.1 may also contribute to its inability to alter calcium current density.

To confirm that γ_6 also interacts with LVA calcium channels in native cells, an adenovirus encoding FLAG tagged γ_6 was added to acute cultures of rat atrial myocytes. Cell lysates were immunoprecipitated with FLAG

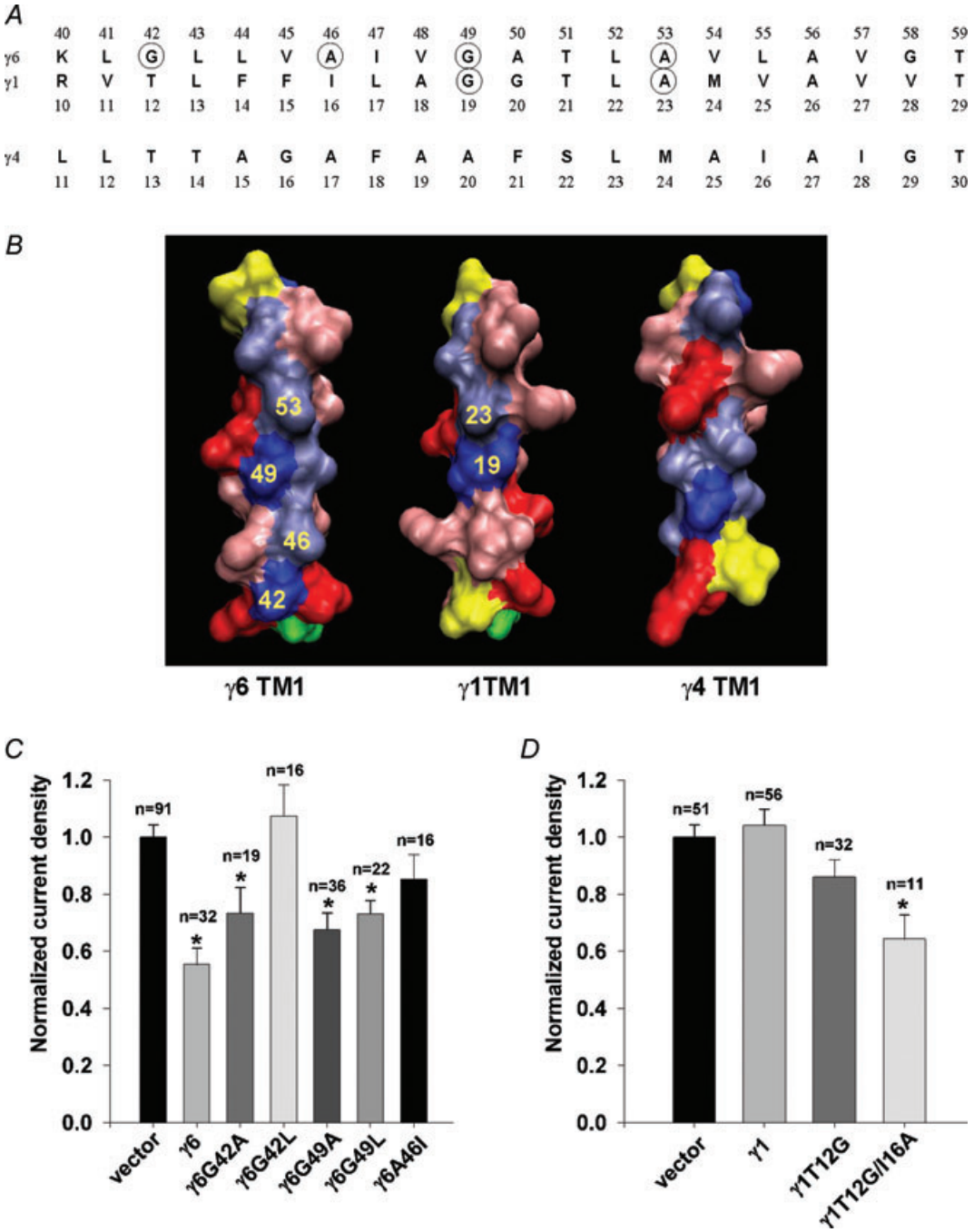

Figure 3. The first GxxxA motif in TM1 of γ_6 is necessary for the effect of the subunit on Cav3.1 current density

A, sequence alignments of TM1 of γ_6, γ_4 and γ_1. TM1 of γ_6 contains two unique GxxxA motifs starting at positions Gly42 and Gly49. TM1 of γ_1 contains only a single GxxxA motif starting at position Gly19. The residues mutated in the study are circled. *B*, theoretical space filling models of the same sequences (G in blue, A in ice blue) illustrating the groove formed by the small side chains along one face of the helix in γ_6. The models were created using the Visual Molecular Dynamics (VMD) software available at http://www.ks.uiuc.edu/Research/vmd/. *C*, normalized, averaged data showing the effects of various point mutations on the ability of γ_6 to decrease Cav3.1 current. Substitution of residues with large side chains at positions Gly42, and Ala46 remove the ability of the subunit to alter current. *D*, introduction of a GxxxA motif into TM1 of γ_1 gives it the ability to decrease Cav3.1 calcium current.

antibody and then probed with anti-Cav3.1 antibody to identify $\gamma_6/\alpha 3.1$ complexes. The result demonstrated a robust co-immunoprecipitation of γ_6 with $\alpha 3.1$ in cardiomyocytes (Fig. 4*C*), suggesting a strong interaction between these two calcium channel subunits under physiological conditions.

In light of the finding that the first GxxxA motif in TM1 of γ_6 is responsible for its inhibitory effect on Cav3.1 current (Fig. 3), we asked if the GxxxA motif is also required for binding of $\gamma_6/\alpha 3.1$ revealed by co-immunoprecipitation. In these experiments we used the FLAGγ_6G42L construct, which we have shown previously to be functionally ineffective in reducing calcium current (Fig. 3*C*). FLAGγ_6G42L binds as strongly as FLAGγ_6 (Fig. 4*A*). This result indicates that the first GxxxA motif in γ_6 TM1, although necessary for the inhibition of Cav3.1 current, is not required for the physical association between γ_6 and $\alpha 3.1$ as probed by co-immunoprecipitation.

Single channel analysis reveals that γ_6 reduces Cav3.1 current by altering channel availability

To better understand the mechanism of inhibition of Cav3.1 currents by the γ_6 subunit, we performed single-channel patch-clamp experiments. Cav3.1 mock-co-transfected with either AdCGI or pGFP vectors served as a reference. As an additional negative control, we used Cav3.1 co-transfected with the γ_7 subunit, which produces no significant effect on Cav3.1 current in the whole-cell experiments (Hansen *et al.* 2004). Typical single-channel recordings are shown in Fig. 5, and the data analysis is summarized in Table 2. The measurements were performed by depolarizing the cell membrane to −20 mV, which is close to the current density peak in whole-cell experiments. The γ_6 subunit inhibited Cav3.1 currents by reducing the channel availability (see below), but did not affect other gating parameters and the unitary current amplitude. As expected, there were no significant differences in single-channel characteristics of Cav3.1 co-transfected with AdCGI, pGFP or γ_7.

Co-transfection of Cav3.1 and γ_6 at a 1 : 1 DNA mass ratio, led to the reduction of the channel availability by ∼22%, which was not statistically significant. At the same time, the distribution of the channel availabilities became wider (Fig. 5). This suggests that not all Cav3.1 channels interacted with γ_6 subunits. Therefore, we increased the amount of γ_6 vector to yield a DNA mass ratio of 1 : 3. Indeed, at these conditions, the width of the channel availability distribution decreased, suggesting a more homogeneous ensemble (Fig. 5). The average channel availability was reduced by 40% from its control value. The difference was significant ($P < 0.05$) compared with Cav3.1 + AdCGI, Cav3.1 + pGFP, and Cav3.1 + γ_7. When all five groups were compared (including potentially heterogeneous Cav3.1 + γ_6, co-transfected at a 1 : 1 DNA mass ratio), the *P*-value was 0.06. Linear regression analysis also confirmed a statistically significant effect of γ_6 on the channel availability ($P < 0.01$).

To increase sample sizes, we pooled data from Cav3.1 + AdCGI and Cav3.1 + pGFP into a single Cav3.1 group, and data from Cav3.1 + γ_6 (1 : 1) and Cav3.1 + γ_6 (1 : 3) into a single Cav3.1 + γ_6 group (Table 2). In the pooled data, γ_6 reduced the channel availability by 28%. The difference was significant as compared with Cav3.1 and Cav3.1 + γ_7 ($P < 0.05$).

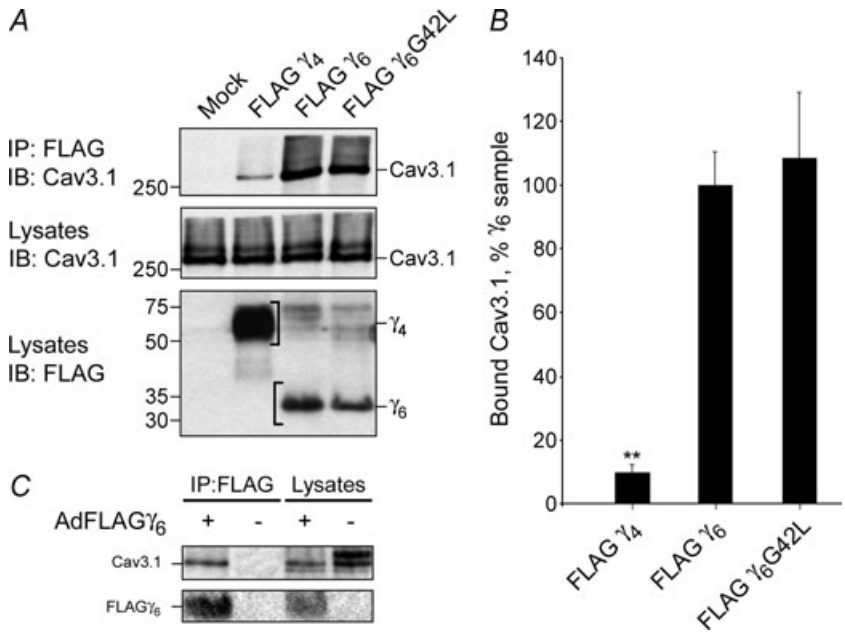

Figure 4. γ_6 co-immunoprecipitates with Cav3.1
A, HEK/Cav3.1 cells were transfected with plasmids containing either FLAG-tagged γ_6 or FLAG-tagged γ_4. After transfection (24 h), cells were lysed and immunoprecipitated (IP) with anti-FLAG M2 beads. Immunoblot (IB) analysis was performed with anti-Cav3.1 and anti-FLAG antibodies. *B*, the bar graph represents a quantification of immunoprecipitated Cav3.1, normalized to the amount of FLAGγ_4, FLAGγ_6, or FLAGγ_6G42L immunoprecipitated from the same sample. The graph depicts the average obtained for a given sample across 4 independent trials, scaled such that the FLAGγ_6 group represents 100%. Binding of γ_6 to Cav3.1 is robust compared to relatively weak binding of γ_4. ($P < 0.01$). *C*, acutely isolated atrial myocytes were infected with adenovirus expressing FLAG-tagged γ_6. After infection (48 h), cells were treated for immunoprecipitation assay as described for panel *A*. Cav3.1 co-immunoprecipitates with γ_6 in atrial myocytes.

The decrease of the channel availability by γ_6 led to reduction of the average current through single Cav3.1 channels (Fig. 5, Table 2), although the difference was not statistically significant because of the large scattering of the data. The shape of the current response remained unaffected, consistent with the whole-cell measurements.

Then we focused on the dynamics of the transitions between available and non-available states. For this, we performed a runs analysis, defining 'run' as a sequence of sweeps, which are all either active or blank. In about 30% of measurements in either Cav3.1 or Cav3.1 + γ_6 groups, the number of runs was significantly less than the number of runs expected for a random sequence ($Z_R > 1.64$, corresponding to $P < 0.05$). This suggests clustering of active and/or blank sweeps resulting from slow dynamics of the transitions between available and non-available states. Mean Z_R values for each group were also significantly larger than 0 ($P < 0.05$). Assuming for simplicity a single available (A) and a single non-available (N) state, we estimated the lifetimes of the available and non-available gating modes (Table 3). For this, average length of blank runs and channel availability were used as described in Methods. The evaluated lifetime of the available state was on a subsecond time scale, which is shorter than the time between voltage test pulses. The lifetime of the non-available state was about two pacing periods. Interaction of Cav3.1 with γ_6 led to a further reduction of the lifetime of the available state as well as to a lengthening of the lifetime of the non-available state.

In addition to the detailed analysis of the channel gating at −20 mV, we tested whether the γ_6 subunit affects channel conductance. For this, we employed HEK 293 cells stably expressing Cav3.1 channels. The conductance values were estimated by linear regression of the unitary current

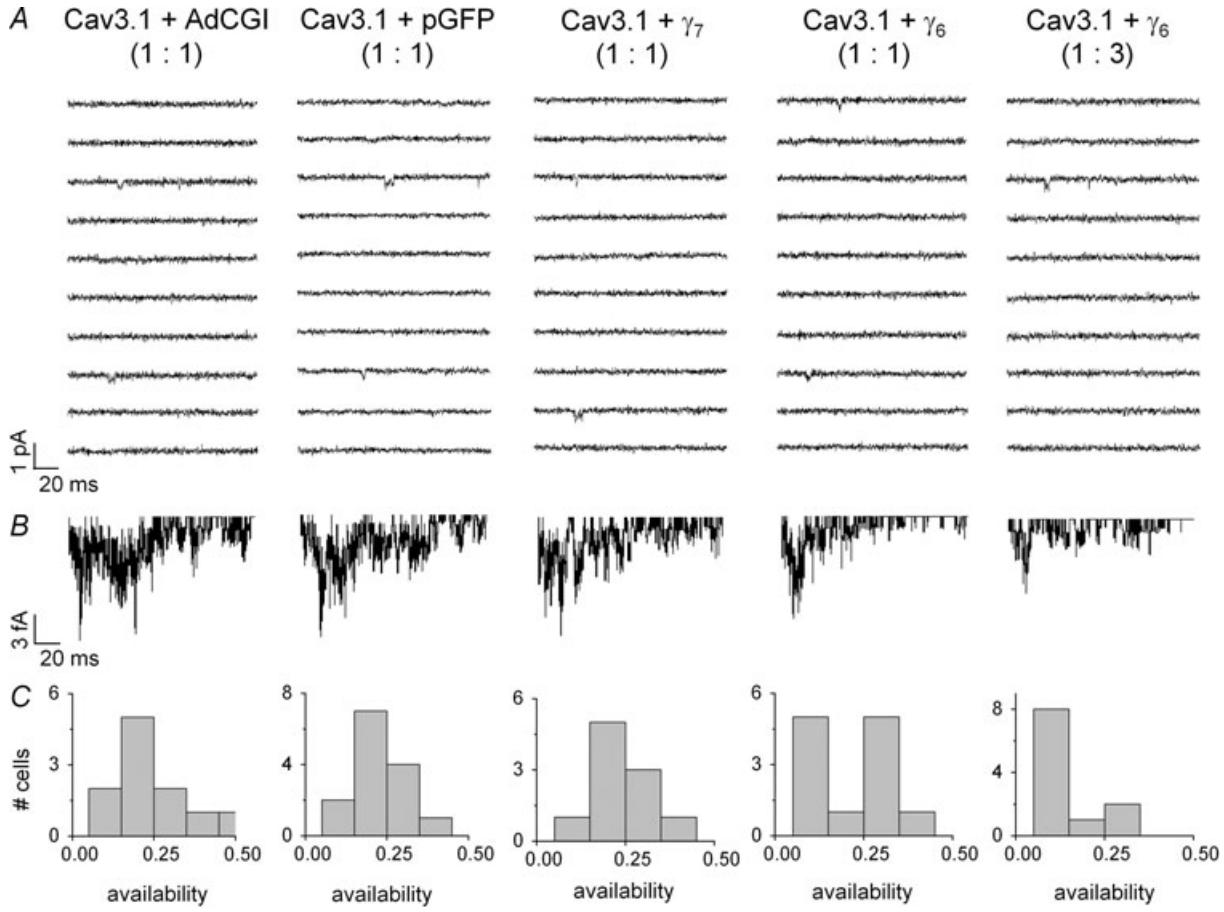

Figure 5. At the single-channel level, γ_6 reduces availability of LVA calcium channels
HEK 293 cells were transiently transfected with Cav3.1 and AdCGI, pGFP, γ_7 or γ_6 vectors. The DNA mass ratio used for the transfection is given in brackets. Barium currents were elicited by a 147.9 ms voltage step to −20 mV from a holding potential of −90 mV. *A* and *B*, representative single channel recordings. *A*, 10 consecutive sweeps. *B*, averages of 60 consecutive sweeps. γ_6 produced a pronounced reduction of the average current without kinetic changes, consistent with whole-cell measurements. *C*, distribution of the channel availabilities revealed heterogeneity of Cav3.1 + γ_6 (1 : 1) sample, indicating that not all Cav3.1 channels had γ_6 bound. In the Cav3.1 + γ_6 (1 : 3) sample, the distribution shifted to the lower availability values and became narrow.

Table 2. γ_6 subunit reduces availability of Cav3.1 channels, while other single channel characteristics remains unaltered

	Cav3.1 + AdCGI (1 : 1)	Cav3.1 + pGFP (1 : 1)	Cav3.1 + γ_7 (1 : 1)	Cav3.1 + γ_6 (1 : 1)	Cav3.1 + γ_6 (1 : 3)
f	0.25 ± 0.03	0.23 ± 0.02	0.24 ± 0.02	0.19 ± 0.03	0.15 ± 0.02
$P_{O,active}$	0.025 ± 0.002	0.031 ± 0.003	0.025 ± 0.004	0.024 ± 0.004	0.034 ± 0.005
I_{peak} (fA)	6.8 ± 1.3	6.5 ± 1.1	6.6 ± 1.2	6.0 ± 1.5	5.1 ± 1.0
inactivation (%)	67 ± 5	62 ± 5	62 ± 5	53 ± 6	56 ± 5
i_O (pA)	0.466 ± 0.005	0.474 ± 0.004	0.476 ± 0.005	0.470 ± 0.006	0.470 ± 0.005
t_O (ms)	0.51 ± 0.02	0.53 ± 0.03	0.57 ± 0.03	0.50 ± 0.02	0.53 ± 0.03
average n_{ch}	1.9 ± 0.2	2.4 ± 0.1	1.7 ± 0.1	1.9 ± 0.1	2.0 ± 0.1
n (all experiments, $n_{ch} \leq 3$)	11	14	10	12	11
n ($n_{ch} = 1$)	2	0	3	2	1

	Cav3.1 pooled	Cav3.1 + γ_7	Cav3.1 + γ_6 pooled
f	0.24 ± 0.02	0.24 ± 0.02	0.17 ± 0.02*
$P_{O,active}$	0.028 ± 0.002	0.025 ± 0.004	0.029 ± 0.003
I_{peak} (fA)	6.7 ± 0.8	6.6 ± 1.2	5.5 ± 0.9
inactivation (%)	64 ± 4	62 ± 5	54 ± 4
$i_{O\ (}$pA)	0.470 ± 0.003	0.476 ± 0.005	0.470 ± 0.004
t_O (ms)	0.52 ± 0.02	0.57 ± 0.03	0.52 ± 0.02
average n_{ch}	2.2 ± 0.1	1.7 ± 0.1	2.0 ± 0.1
n (all experiments, $n_{ch} \leq 3$)	25	10	23
n ($n_{ch} = 1$)	2	3	3

All data are expressed as mean ± S.E.M. The upper and the lower parts of the table presents comparison between individual and pooled groups, respectively. Channel availability was significantly reduced by γ_6 subunit as compared to cells with no and with γ_7 subunits (pooled data, $P < 0.05$). No significant differences in other gating parameters and a unitary current through a Cav3.1 channel were detected. * $P < 0.05$

Table 3. Availability/nonavailability of Cav3.1 channels results from slow transitions between different kinetic states

	Cav3.1 + AdCGI (1 : 1)	Cav3.1 + pGFP (1 : 1)	Cav3.1 + γ_6 (1 : 1)	Cav3.1 + γ_6 (1 : 3)	Cav3.1 pooled	Cav3.1 + γ_6 pooled
Z_R	1.2 ± 0.4**	1.1 ± 0.3**	1.2 ± 0.5*	1.1 ± 0.4**	1.1 ± 0.2***	1.2 ± 0.3***
τ_A (s)	0.9 ± 0.2	0.9 ± 0.1	0.9 ± 0.2	0.7 ± 0.2	0.9 ± 0.1	0.8 ± 0.1
τ_N (s)	3.5 ± 0.8	3.5 ± 0.7	4.3 ± 1.5	4.6 ± 1.2	3.5 ± 0.5	4.5 ± 0.9
n	11	14	12	11	25	23

All data are expressed as mean ± S.E.M. Number of runs in single channel recordings was significantly lower than the expected number for random occurrence of the active and blank sweeps ($Z_R > 0$), indicating a clustering of sweeps with a particular gating mode. *$P < 0.05$, **$P < 0.01$, and ***$P < 0.001$ to test $Z_R > 0$.

amplitude against pulse voltage. The conductance values were the same without and with γ_6 (6.5 ± 1.0 pS, $n = 3$; and 6.2 ± 0.80 pS, $n = 3$, respectively).

Summing up, single-channel analysis revealed that γ_6 significantly reduced availability of Cav3.1 channels, resulting from both a destabilization of the available and a stabilization of the non-available states.

The γ_6 subunit alters LVA calcium current in atrial myocytes

Finally, to test whether γ_6 is capable of modulating LVA calcium current under more physiological conditions, we engineered an adenovirus expressing FLAG tagged γ_6 and used it to over-express γ_6 in cultured atrial myocytes (Fig. 6*A*). LVA and HVA calcium density were then measured electrophysiologically (Fig. 6*B*).

Over-expressing γ_6 significantly reduced LVA, but not HVA, calcium current density in these myocytes confirming that current inhibition by γ_6 occurs physiologically and that it is selective in altering only LVA current (Fig. 6*C* and *D*).

Discussion

A GxxxA motif required for γ_6 inhibition of Cav3.1 current

This work provides direct evidence that γ_6 modulates LVA calcium current in cardiac myocytes. Using both chimeric proteins and site directed mutagenesis we have identified a specific GxxxA motif within γ_6 located near the cytoplasmic end of the first transmembrane domain (TM1) of the protein that is required for this inhibitory effect.

Arikkath and colleagues have previously investigated the ability of γ_1 to reduce HVA calcium currents using γ_1–γ_2 chimeras. There is strong biochemical evidence supporting the existence of γ_1–α1.1 complexes in native cells and functional assays clearly demonstrate a pronounced inhibitory effect of γ_1 on HVA calcium currents (Freise *et al.* 2000; Held *et al.* 2002; Arikkath *et al.* 2003). γ_2, one of the TARPs, however, does not have any functional effect on Cav1.1 current. Arikkath

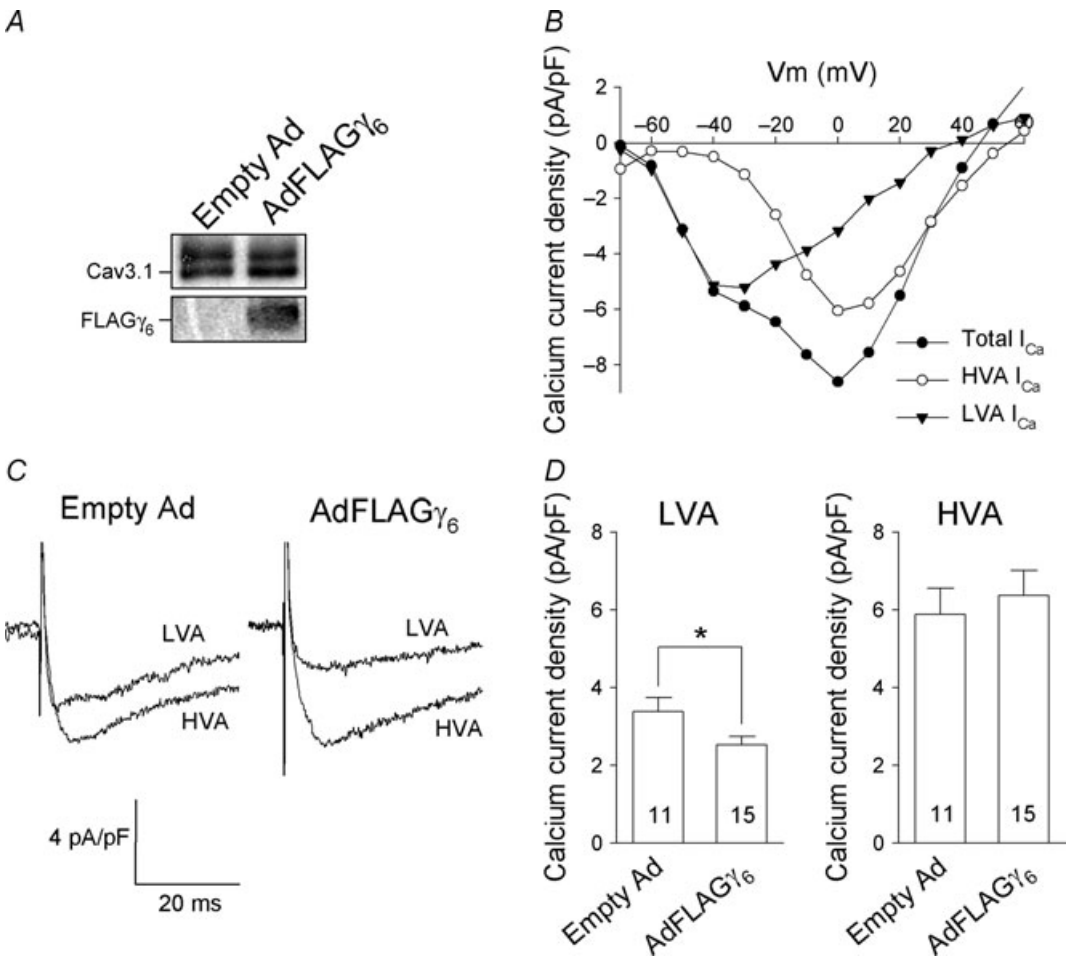

Figure 6. γ_6 inhibits LVA calcium currents in native atrial myocytes
A, demonstration of equal Cav3.1 expression levels following adenovirus treatment at optimized multiplicity of infection for the electrophysiological assay. *B*, current–voltage relationships from a cultured atrial myocytes 48 h after being infected with empty adenovirus. Total calcium currents were elicited from holding potential of −100 mV. HVA calcium currents were elicited from a holding potential of −50 mV. LVA currents were measured using the difference traces obtained by subtracting the HVA from the total I_{Ca} traces. Notably the total I_{Ca} at −40 mV is essentially the LVA I_{Ca} at the same voltage. *C*, representative LVA (at −40 mV) and HVA (at 0 mV) calcium currents from two atrial myocytes infected, respectively, with empty adenovirus and adenovirus expressing FLAGγ_6. *D*, average LVA and HVA calcium current densities in atrial myocytes infected with empty adenovirus or adenovirus expressing FLAGγ_6. Over-expressing FLAGγ_6 in myocytes significantly reduces only LVA, but not HVA, calcium currents densities ($P < 0.05$).

and Campbell showed that a chimera containing the N-terminal half of γ_1 and the C-terminal half of γ_2 possesses the same functionality as the γ_1 subunit in both a heterologous expression system and in native γ_1 –/– mouse myotubes (Arikkath *et al.* 2003). However, chimeras containing the N-terminal half of γ_2 and the C-terminal half of γ_1 were not inhibitory. They concluded that the critical motif(s) controlling the effects of γ_1 on Cav1.1 current must be contained in the N-terminal half of the protein. This result is consistent with our data on γ_6 and its effects on Cav3.1 current showing that the critical domain is TM1.

GxxxG and related motifs enhance helix–helix interactions in both soluble and membrane associated proteins (Russ & Engelman, 2000; Curran & Engelman, 2003; Senes *et al.* 2004). The presence of amino acids with small side chains (G, A, or S) located three residues (one helical turn) apart creates on one helical face an area that permits close contact with a neighbouring helix. It is thought that this close association then allows the formation of hydrogen bonds or van der Waals interactions (Kleiger & Eisenberg, 2002). While the presence of a GxxxG or related motif can promote helical interactions, the presence of suitable near neighbour residues is also crucial for the formation of stable complexes (Schneider & Engelman, 2004; Kobus & Fleming, 2005). Senes and colleagues have shown that the GxxxG motif frequently occurs with neighbouring branching residues (V, I, L) at adjoining positions (± 1) and have proposed that they may be critical for helix–helix interactions or in modulating helix flexibility (Senes *et al.* 2000). Thus while the GxxxG or related motif creates an appropriate contact surface, side chain interactions are also critical for determining the stability of any helix–helix associations (Schneider, 2004).

The GxxxA motifs found in TM1 of the γ_6 calcium channel subunits of rat, mouse and human conform to the classical description of these helical interaction domains (for sequence comparisons, see Chu *et al.* 2001). By definition, each motif contains two residues with small side chains separated by three intervening residues (GxxxA) and each motif is accompanied by residue(s) with a branching side chain (for rat: $LG^{42}LxVA^{46}I$; $VG^{49}xxLA^{53}V$). In TM1 of human γ_6 the first motif becomes LALxLAx while the second motif is identical to that of rat and mouse (VGxxLAV). Thus there is a high degree of sequence conservation amongst species for these motifs in the γ_6 subunit. It is interesting that while TM1 of γ_4 does contain overlapping AxxxA and GxxxA motifs they are more centrally located and neither is associated with a residue containing a branching side chain. Whether this difference underlies γ_4's inability to bind robustly to α3.1 and to alter calcium current remains to be investigated.

Despite being the closest homologue to γ_6, the γ_1 subunit does not alter Cav3.1 calcium current in our heterologous expression system (Fig. 3*D*). This result is consistent with a recent report that γ_1 has no effect on Cav3.2 current (Sandoval *et al.* 2007). These data suggest that the γ_1 and γ_6 subunits are capable of selectively targeting HVA and LVA channels. How might this selectivity occur? The γ_6 subunit contains two GxxxA motifs in TM1 while γ_1 contains only one. Only the GxxxA motif near the cytoplasmic end of γ_6 TM1 ($G^{42}xxxA^{46}$) is required for its inhibitory effect on Cav3.1 current. The GxxxA motif in TM1 of γ_1 is located near the extracellular end of the domain in a position homologous to the non-critical motif in γ_6. Thus one possible answer is that the position of the motif within TM1 determines the identity of the subunit's target. If this is correct then introduction of a second GxxxA motif near the cytoplasmic end of TM1 should allow it to inhibit Cav3.1 calcium current. This is exactly what occurred with the γ_1 subunit containing the double mutation (T12G, I16A; see Fig. 3*D*).

There is a major distinction, though, between the characteristics of action of γ_1 and γ_6 on calcium current. γ_1 reduces Ca^{2+} influx mainly by accelerating channel inactivation (Freise *et al.* 2000) and causing a hyperpolarizing shift of the inactivation curve (Freise *et al.* 2000; Held *et al.* 2002; Ursu *et al.* 2004; Andronache *et al.* 2007). Although γ_1 can also decrease HVA current density, this effect is limited to myotubes less than 4 weeks old, and appears to be independent from the effect on voltage dependence of inactivation (Held *et al.* 2002). In contrast, our results indicate that γ_6 only affects current density, but not voltage dependence of inactivation, of the LVA Ca^{2+} current. Our single channel data provide crucial evidence that γ_6 modulates Cav3.1 channel gating in a different way than γ_1 interacts with Cav1.1 channel. Consistent with this notion, we also show that γ_1 does not modulate Cav3.1 current like γ_6 (Fig. 3*D*), while γ_6 selectively inhibits LVA, but not HVA, currents in myocytes (Fig. 6*C* and *D*). These observations speak to the functional differentiation and evolutionary diversification within the γ family (Chen *et al.* 2007).

Direct γ_6/α3.1 interaction as shown by co-immunoprecipitation

Our co-immunoprecipitation experiments have demonstrated that γ_6 forms stable complexes with α3.1 (Fig. 4) in both HEK cells and atrial myocytes. However, the location of the binding site on α3.1 is yet to be identified. While we have shown that a unique GxxxA motif in γ_6 TM1 is necessary for current inhibition, co-immunoprecipitation studies using the non-functional FLAGγ_6G42L mutant indicates that the association between γ_6 and α3.1 requires sequences other than the functional GxxxA motif (Fig. 4*A*). Interestingly, it has been shown in the group of γ subunits referred

to as the TARPs that the site required for physical clustering with the main pore-forming subunit of the AMPA receptor is different from the site responsible for functionally modulating its properties (Tomita *et al.* 2005).

Mechanisms of action

The major functional effect of the γ_6 subunit is to decrease LVA calcium current density with little or no

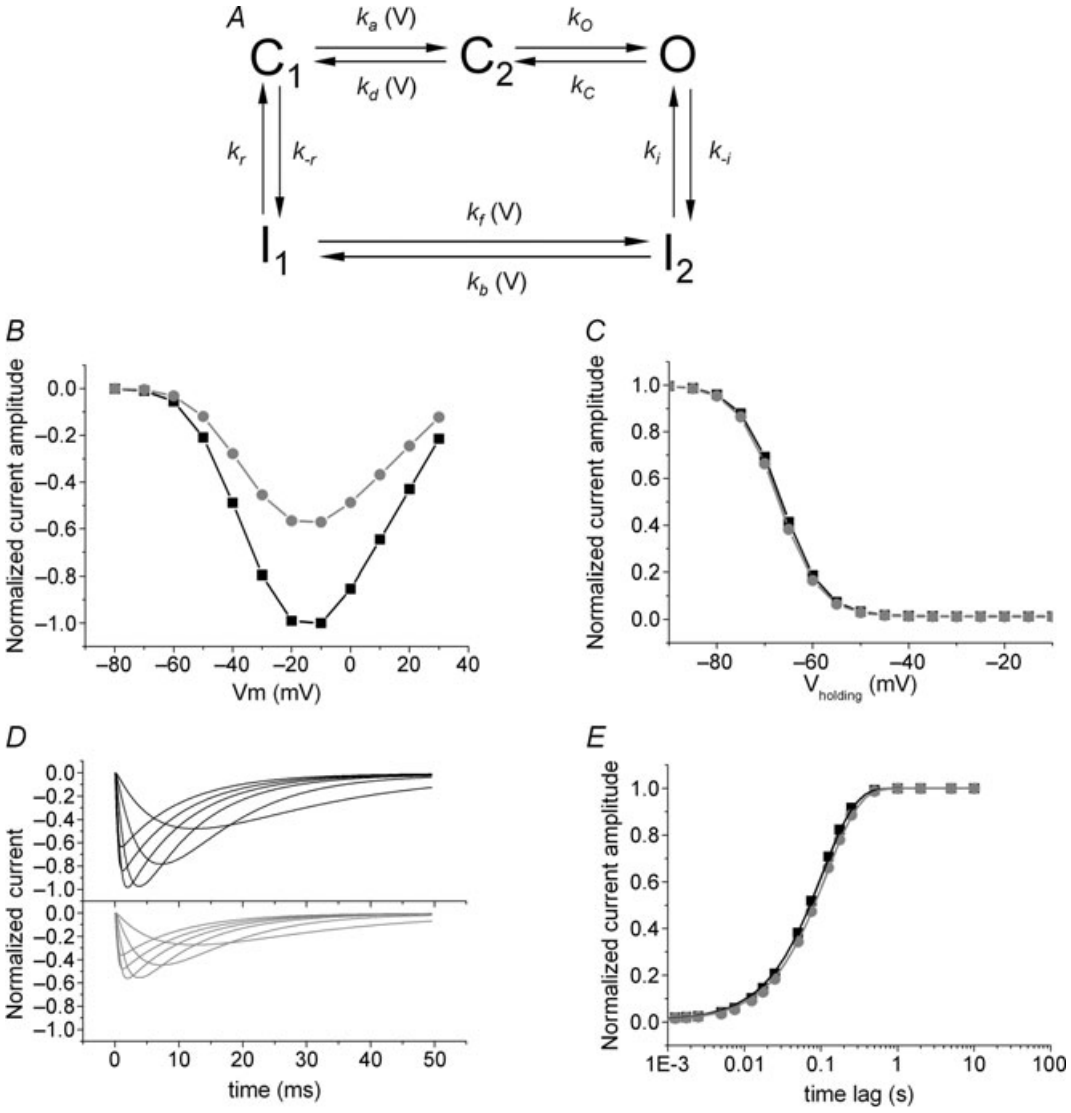

Figure 7. Model simulations
A, simplified gating scheme of T-type Ca^{2+} channels, used in our simulations (after Chen & Hess, 1990). The model describes transition between closed (C), open (O) and inactivated (I) states. k_a, k_d, k_f and k_b rates are voltage dependent; other rates are voltage independent. At the resting potential channels are in equilibrium between C_1 and I_1 states. The fraction of channels in C_1 state, $k_r/(k_r + k_{-r})$, determines channel availability for activation. *B–E*, whole-cell currents were simulated by numerical solution of differential equations describing channel gating by using home-made software IonFit (Kuzmenkin *et al.* 2007*a*,*b*). Microscopic rate parameters were taken from Chen & Hess (1990) (data shown in black) or, alternatively, microscopic recovery rates (k_r and k_{-r}) were reduced by a factor of two as compared to their original values (data shown in grey). In our simulations, the reduction of microscopic recovery rates led to reduction of the current density, while other whole-cell characteristics remained unchanged. *B*, *I–V* curve was constructed by taking current peaks at different test potentials stepping from the resting potential of −100 mV. *C*, steady-state inactivation curve was calculated by taking current peaks at the test potential of −20 mV stepping from the different holding potentials. *D*, examples of simulated currents. Currents were elicited by voltage step to −40 to +10 mV from the holding potential of −100 mV. *E*, macroscopic recovery was calculated as follows. First, channels were inactivated by holding at −20 mV. Second, channels were let to recover for a given time by stepping membrane voltage to −100 mV. Then, current amplitudes were calculated from the test pulse to −20 mV. Current amplitudes are plotted against the recovery time and fitted by a single exponent.

effect on current voltage dependency or kinetics. A simple explanation for its effects is that the subunit reduces the number of functional channels in the plasma membrane either from charge immobilization or from a decrease in channel number (Sandoval *et al.* 2007). Our single channel analysis strongly disfavours the second hypothesis. We showed that upon interaction with γ_6, Cav3.1 channels remained functional but the channel availability was reduced. The magnitude of the effect was dependent on the amount of γ_6 transfected. When the DNA mass ratio of 1 : 3 (Cav3.1 : γ_6) was used, the channel availability was reduced by ∼40%, in agreement with the current density reduction by γ_6 measured in whole-cell experiments.

The molecular basis of the non-available gating mode of LVA calcium channels remains to be clarified. Interaction with γ_6 resulted in the apparent increase of the transition rate from the available to the non-available gating mode as well as in the longer trapping of the channel in the non-available state. It is possible that γ_6 causes conformational changes of Cav3.1, which lead to the changes of free energies between its available and non-available states.

It was proposed that single-channel non-availability of T-type calcium channels results from the closed-state inactivation (for review see Perez-Reyes, 2003). We tested whether simple changes in the closed-state inactivation can reproduce our whole-cell observations, i.e. can cause the reduction of the current density without significant changes in the shape of *I–V* and steady-state inactivation curves. We turned to a simple model proposed by Chen & Hess (Fig. 7*A*), which fairly described their whole-cell and single-channel data (Chen & Hess, 1990). First, we performed simulation of whole-cell currents using the same model rate parameters as in the original paper. Second, we reduced microscopic recovery rates (i.e. k_r and k_{-r}) by the same factor. This corresponds to the lowering of the free-energy values of inactivated states by an equal amount. Indeed, the reduction of the microscopic recovery rates by a factor of 2 resulted in the reduction of the current density by about 40%, and the shape of *I–V* and steady-state inactivation curves remained unchanged (Fig. 7*B* and *C*). As expected, no changes in the activation and inactivation rates were found in simulated currents (Fig. 7*D*). Moreover, there were virtually no changes in macroscopic recovery rates, which were reduced only by *ca* 10% (Fig. 7*E*).

Alternatively, the interaction with γ_6 may lead to a formation of an additional non-available conformation. Our kinetic analysis reveals that the lifetime of this conformation is not much longer than 4.6 s, the apparent lifetime of the non-available state in Cav3.1 + γ_6 (1 : 3) sample. A more-detailed examination of the question was hindered by a short lifetime of the available state (below the time between two sweeps).

Our results reinforce the idea that members of the calcium channel γ subunit family may perform multiple functions within cells (Chen *et al.* 2007). The proposed function of members of this family of proteins was originally defined by the properties of γ_1 which associates with and alters the properties of the HVA current in skeletal muscle (Freise *et al.* 2000; Arikkath *et al.* 2003). More recently the four isoforms containing PDZ-binding motifs (γ_2, γ_3, γ_4 and γ_8) have been shown to play major physiological roles as auxiliary subunits of AMPA receptors rather than as subunits of calcium channels (Tomita *et al.* 2003; Vandenberghe *et al.* 2005). They are involved in transport, targeting and anchoring of AMPA receptors and may also modulate their biophysical properties (Osten & Stern-Bach, 2006). The γ_2 isoform has also been shown to modify cell aggregation (Price *et al.* 2005). In contrast, while neither γ_1 nor γ_6 is known to alter AMPA receptor trafficking or function, both isoforms have been shown (by co-immunoprecipitation) to form complexes with α_1 subunits of calcium channels and both dramatically alter calcium current density.

References

Andronache Z, Ursu D, Lehnert S, Freichel M, Flockerzi V & Melzer W (2007). The auxiliary subunit gamma 1 of the skeletal muscle L-type Ca^{2+} channel is an endogenous Ca^{2+} antagonist. *Proc Natl Acad Sci U S A* **104**, 17885–17890.

Arikkath J, Chen CC, Ahern C, Allamand V, Flanagan JD, Coronado R, Gregg RG & Campbell KP (2003). γ1 subunit interactions within the skeletal muscle L-type voltage-gated calcium channels. *J Biol Chem* **278**, 1212–1219.

Burgess DL, Gefrides LA, Foreman PJ & Noebels JL (2001). A Cluster of three novel Ca^{2+} channel gamma subunit genes on chromosome 19q13.4: evolution and expression profile of the gamma subunit gene family. *Genomics* **71**, 339–350.

Chen R-S, Deng T-C, Garcia T, Sellers ZM & Best PM (2007). Calcium channel γ subunits: a funtionally diverse protein family. *Cell Biochem Biophys* **47**, 178–186.

Chen CF & Hess P (1990). Mechanism of gating of T-type calcium channels. *J Gen Physiol* **96**, 603–630.

Chu PJ, Robertson HM & Best PM (2001). Calcium channel gamma subunits provide insights into the evolution of this gene family. *Gene* **280**, 37–48.

Curran AR & Engelman DM (2003). Sequence motifs, polar interactions and conformational changes in helical membrane proteins. *Curr Opin Struct Biol* **13**, 412–417.

Eberst R, Dai S, Klugbauer N & Hofmann F (1997). Identification and functional characterization of a calcium channel γ subunit. *Pflugers Arch* **433**, 633–637.

Freise D, Held B, Wissenbach U, Pfeifer A, Trost C, Himmerkus N, Schweig U, Freichel M, Biel M, Hofmann F, Hoth M & Flockerzi V (2000). Absence of the gamma subunit of the skeletal muscle dihydropyridine receptor increases L-type Ca^{2+} currents and alters channel inactivation properties. *J Biol Chem* **275**, 14476–14481.

Hansen JP, Chen RS, Larsen JK, Chu PJ, Janes DM, Weis KE & Best PM (2004). Calcium channel γ6 subunits are unique modulators of low voltage-activated (Cav3.1) calcium current. *J Mol Cell Cardiol* **37**, 1147–1158.

Held B, Freise D, Freichel M, Hoth M & Flockerzi V (2002). Skeletal muscle L-type Ca^{2+} current modulation in γ1-deficient and wildtype murine myotubes by the γ1 subunit and cAMP. *J Physiol* **539**, 459–468.

Horn R, Vandenberg CA & Lange K (1984). Statistical analysis of single sodium channels. Effects of N-bromoacetamide. *Biophys J* **45**, 323–335.

Jay SD, Ellis SB, McCue AF, Williams ME, Vedvick TS, Harpold MM & Campbell KP (1990). Primary structure of the γ subunit of the DHP-sensitive calcium channel from skeletal muscle. *Science* **248**, 490–492.

Kleiger G & Eisenberg D (2002). GXXXG and GXXXA motifs stabilize FAD and NAD(P)-binding Rossmann folds through C_α-H. . .O hydrogen bonds and van der waals interactions. *J Mol Biol* **323**, 69–76.

Kobus FJ & Fleming KG (2005). The GxxxG-containing transmembrane domain of the CCK4 oncogene does not encode preferential self interactions. *Biochemistry* **44**, 1464–1470.

Kuzmenkin A, Hang C, Kuzmenkina E & Jurkat-Rott K (2007*a*). Gating of the HypoPP-1 mutations: I. Mutant-specific effects and cooperativity. *Pflugers Arch* **454**, 495–505.

Kuzmenkin A, Hang C, Kuzmenkina E & Jurkat-Rott K (2007*b*). Gating of the HypoPP-1 mutations: II. Effects of a calcium-channel agonist BayK 8644. *Pflugers Arch* **454**, 605–614.

Michels G, Matthes J, Handrock R, Kuchinke U, Groner F, Cribbs LL, Pereverzev A, Schneider T, Perez-Reyes E & Herzig S (2002). Single-channel pharmacology of mibefradil in human native T-type and recombinant $Ca_v3.2$ calcium channels. *Mol Pharmacol* **61**, 682–694.

Nilius B (1988). Modal gating behavior of cardiac sodium channels in cell-free membrane patches. *Biophys J* **53**, 857–862.

Osten P & Stern-Bach Y (2006). Learning from stargazin: the mouse, the phenotype and the unexpected. *Curr Opin Neurobiol* **16**, 275–280.

Perez-Reyes E (2003). Molecular physiology of low-voltage-activated t-type calcium channels. *Physiol Rev* **83**, 117–161.

Piedras-Renteria ES, Chen CC & Best PM (1997). Antisense oligonucleotides against rat brain α1E DNA and its atrial homologue decrease T-type calcium current in atrial myocytes. *Proc Natl Acad Sci U S A* **94**, 14936–14941.

Price MG, Davis CF, Deng F & Burgess DL (2005). The α-amino-3-hydroxyl-5-methyl-4-isoxazolepropionate receptor trafficking regulator 'stargazin' is related to the claudin family of proteins by its ability to mediate cell-cell adhesion. *J Biol Chem* **280**, 19711–19720.

Russ WP & Engelman DM (2000). The GxxxG motif: a framework for transmembrane helix–helix association. *J Mol Biol* **296**, 911–919.

Sandoval A, Arikkath J, Monjaraz E, Campbell KP & Felix R (2007). γ_1-dependent down-regulation of recombinant voltage-gated Ca^{2+} channels. *Cell Mol Neurobiol* **27**, 901–908.

Schneider D (2004). Rendezvous in a membrane: close packing, hydrogen bonding, and the formation of transmembrane helix oligomers. *FEBS Lett* **577**, 5–8.

Schneider D & Engelman DM (2004). Motifs of two small residues can assist but are not sufficient to mediate transmembrane helix interactions. *J Mol Biol* **343**, 799–804.

Senes A, Engel DE & DeGrado WF (2004). Folding of helical membrane proteins: the role of polar, GxxxG-like and proline motifs. *Curr Opin Struct Biol* **14**, 465–479.

Senes A, Gerstein M & Engelman DM (2000). Statistical analysis of amino acid patterns in transmembrane helices: the GxxxG motif occurs frequently and in association with β-branched residues at neighboring positions. *J Mol Biol* **296**, 921–936.

Singer D, Biel M, Lotan I, Flockerzi V, Hofmann F & Dascal N (1991). The roles of the subunits in the function of the calcium channel. *Science* **253**, 1553–1557.

Tomita S, Adesnik H, Sekiguchi M, Zhang W, Wada K, Howe JR, Nicoll RA & Bredt DS (2005). Stargazin modulates AMPA receptor gating and trafficking by distinct domains. *Nature* **435**, 1052–1058.

Tomita S, Chen L, Kawasaki Y, Petralia RS, Wenthold RJ, Nicoll RA & Bredt DS (2003). Functional studies and distribution define a family of transmembrane AMPA receptor regulatory proteins. *J Cell Biol* **161**, 805–816.

Ursu D, Schuhmeier RP, Freichel M, Flockerzi V & Melzer W (2004). Altered inactivation of Ca^{2+} current and Ca^{2+} release in mouse muscle fibers deficient in the DHP receptor γ1 subunit. *J Gen Physiol* **124**, 605–618.

Vandenberghe W, Nicoll RA & Bredt DS (2005). Stargazin is an AMPA receptor auxiliary subunit. *Proc Natl Acad Sci U S A* **102**, 485–490.

Acknowledgements

We thank Dr Dorothy A. Hanck and Dr Edward Perez-Reyes for the stable $Ca_v3.1$ HEK cell line. The work was supported by a GIA from the American Heart Association and funds from the University of Illinois to P.M.B.